21st Australasian Fluid Mechanics Conference
Adelaide, Australia
10-13 December 2018

Estimation of Coherent Large-Scale Structures using the Linearized Navier-Stokes Equations

Anagha Madhusudanan[1], Simon. J. Illingworth[1] and Ivan Marusic[1]

[1]Department of Mechanical Engineering
University of Melbourne, Melbourne, VIC 3010, Australia

Abstract

We use the Navier-Stokes equations linearized about the turbulent mean velocity profile to estimate the instantaneous velocity field and 2-D energy spectrum of a turbulent channel flow at a friction Reynolds number of $Re_\tau = 2000$. Spectral linear stochastic estimation is used to build the estimator. The estimator takes as input the instantaneous streamwise velocity field ($\boldsymbol{u}$) or the two-dimensional (2-D) energy spectrum of $\boldsymbol{u}$ at one wall-normal location to provide the estimate of the same quantity at a different wall-normal location. Estimators built using two variations of the linear model are considered here: i) LNS, where the viscosity is equal to the kinematic viscosity and ii) eLNS, where the viscosity is augmented with an eddy viscosity profile. Direct Numerical Simulation (DNS) data from a turbulent channel flow are used to evaluate the estimates obtained from the linear models. The addition of the eddy viscosity profile is found to significantly improve the estimation over a range of wall-heights.

Introduction

In wall-bounded flows, the Navier Stokes equations linearized about the turbulent mean velocity profile gives rise to large-scale coherent structures like those observed in experiments (eg. Del Álamo and Jiménez [2006], McKeon and Sharma [2010], Hwang and Cossu [2010]). This suggests that a linear estimator built using these equations could estimate the statistics of the large-scale structures of the flow. Hence the following question is considered here: given the measurement of the statistics of these structures at one location, can the equations correctly model their features at another location?

The ability of the linearized Navier-Stokes equations to estimate these structures will largely depend on the coherence between the measurement and estimation locations. Hence a coherence based estimation tool, spectral linear stochastic estimation (SLSE) introduced by Tinney et al. [2006], is used here. This technique in conjunction with experimental data was used to estimate the coherent large-scale structures from experiments and further the understanding of these structures [Baars et al., 2016]. Here we use this technique along with the linear models to estimate and understand coherent large-scale structures.

Linear model

A statistically steady incompressible turbulent channel flow at $Re_\tau = 2000$ is considered here. The friction Reynolds number $Re_\tau = u_\tau h/\nu$ is defined using the kinematic viscosity ν of the flow, the channel half-height h and the friction velocity $u_\tau = \sqrt{(\tau_w/\rho)}$, where τ_w is the wall shear stress and ρ is the density of the fluid. The streamwise, spanwise and wall-normal directions are denoted by x, y and z respectively and the corresponding velocity components by u, v and w. The velocities are normalised by u_τ and the spatial variables by h. The pressure fluctuations are p, normalised by ρu_τ^2.

To arrive at a linear model of the flow, the Reynolds decomposition is substituted into the Navier-Stokes equations after which the mean equations are subtracted, hence giving

$$\frac{\partial \boldsymbol{u}}{\partial t} + (\boldsymbol{U}\cdot\nabla)\boldsymbol{u} + (\boldsymbol{u}\cdot\nabla)\boldsymbol{U} + \nabla \boldsymbol{p} - \frac{1}{Re_\tau}\nabla^2\boldsymbol{u} = \boldsymbol{d}, \quad \nabla\cdot\boldsymbol{u} = 0, \tag{1}$$

where $\boldsymbol{U} = (U(z),0,0)$ is the mean velocity profile and $\boldsymbol{u} = (u,v,w)$ denotes fluctuations of the velocity from the mean. Following McKeon and Sharma [2010], all non-linear terms are modelled by a disturbance term $\boldsymbol{d} = -u.\nabla u + \overline{u.\nabla u}$. Here $\boldsymbol{d}$ is assumed to be stochastic and white-in-time [Hwang and Cossu, 2010]. This model is called LNS here.

Equation (1) requires as an input the mean velocity profile of the flow. For convenience, here $U(z)$ is derived from the Cess [1958] eddy viscosity model [Reynolds and Hussain, 1972], which defines a total viscosity $\nu_T(z)$ as the sum of a constant molecular viscosity and a wall-normally varying eddy viscosity. As a function of z, this total viscosity profile is

$$\nu_T(z) = \frac{\nu}{2}\left(1 + \frac{\kappa^2 Re_\tau^2}{9}(2z-z^2)^2(3-4z+z^2)^2 \times \left[1 - exp\left(\frac{-Re_\tau z}{A}\right)\right]^2\right)^{1/2} + \frac{\nu}{2}. \tag{2}$$

The mean velocity profile is obtained by integrating the expression $Re_\tau(1-z)\nu/\nu_T$ in the wall-normal direction. The values of the constants in (2) are taken to be $\kappa = 0.426$ and $A = 25.4$, following Del Álamo and Jiménez [2006], where they were obtained through a least-square fit to experimentally obtained mean velocity profiles at $Re_\tau = 2000$.

A variation of the linear model is obtained by augmenting the kinematic viscosity with an eddy viscosity profile [eg. Del Álamo and Jiménez [2006], Hwang and Cossu [2010]]. Here, this model is called eLNS and is given as

$$\frac{\partial \boldsymbol{u}}{\partial t} + (\boldsymbol{U}\cdot\nabla)\boldsymbol{u} + (\boldsymbol{u}\cdot\nabla)\boldsymbol{U} + \nabla \boldsymbol{p} - \nabla\cdot\left[\frac{\nu_T(z)}{\nu}(\nabla\boldsymbol{u} + \nabla\boldsymbol{u}^T)\right] = \boldsymbol{d}, \quad \nabla\cdot\boldsymbol{u} = 0. \tag{3}$$

As for LNS, the mean velocity profile is obtained from (2). Additionally, the eddy viscosity profile $\nu_T(z)$ is obtained from (2).

A Fourier transformation in the homogeneous streamwise and spanwise directions gives the Fourier coefficients of $\boldsymbol{u}$ and $\boldsymbol{d}$ as $\hat{\boldsymbol{u}}(z,t;k_x,k_y) = (\hat{u},\hat{v},\hat{w})$ and $\hat{\boldsymbol{d}}(z,t;k_x,k_y) = (\hat{d_x},\hat{d_y},\hat{d_z})$, where (k_x,k_y) are the streamwise and spanwise wavenumbers non-dimensionalised by $(1/h)$, and (λ_x,λ_y) the corresponding wavelengths. The Orr-Sommerfeld Squire form of the models (1) and (3) are then [Hwang and Cossu, 2010]

$$\begin{aligned}\dot{\hat{\boldsymbol{q}}} &= \mathbf{A}\hat{\boldsymbol{q}} + \mathbf{B}\hat{\boldsymbol{d}},\\ \hat{\boldsymbol{u}} &= \mathbf{C}\hat{\boldsymbol{q}},\end{aligned} \tag{4}$$

where $\hat{\boldsymbol{q}} = (\hat{w}, \hat{\omega}_z)$ is the vector with the Fourier coefficients of the wall-normal velocity and wall-normal vorticity. The boundary conditions are enforced on both walls as $\hat{w}(\pm h) = \partial\hat{w}(\pm h)/\partial z = \hat{\omega}_z(\pm h) = 0$. The matrices **A**, **B** and **C** for LNS and eLNS in (4) are

$$\mathbf{A}(k_x,k_y) = \begin{bmatrix} \Delta^{-1} & 0 \\ 0 & I \end{bmatrix} \begin{bmatrix} \mathcal{L}_{OS} & 0 \\ -ik_y\boldsymbol{U}' & \mathcal{L}_{SQ} \end{bmatrix}, \tag{5}$$

$$\mathbf{B}(k_x,k_y) = \begin{bmatrix} \Delta^{-1} & 0 \\ 0 & I \end{bmatrix} \begin{bmatrix} -ik_x\mathcal{D} & -ik_y\mathcal{D} & -k^2 \\ ik_y & -ik_x & 0 \end{bmatrix}, \tag{6}$$

$$\mathbf{C}(k_x,k_y) = \frac{1}{k^2} \begin{bmatrix} ik_x\mathcal{D} & -ik_y \\ ik_y\mathcal{D} & ik_x \\ k^2 & 0 \end{bmatrix}. \tag{7}$$

Here $\mathcal{D}$ and $'$ represent differentiation in the wall-normal direction, and $\Delta^2 = \mathcal{D}^2 - k^2$ where $k^2 = k_x^2 + k_y^2$. The matrices $\mathcal{L}_{OS}$ and $\mathcal{L}_{SQ}$ in (5) for LNS are

$$\begin{aligned} \mathcal{L}_{OS} &= -ik_x\boldsymbol{U}\Delta + ik_x\boldsymbol{U}'' + (1/Re)\Delta^2, \\ \mathcal{L}_{SQ} &= -ik_x\boldsymbol{U} + (1/Re)\Delta. \end{aligned} \tag{8}$$

For eLNS the operators are

$$\begin{aligned} \mathcal{L}_{OS} &= -ik_x\boldsymbol{U}\Delta + ik_x\boldsymbol{U}'' + \nu_T\Delta^2 + 2\nu_T'\mathcal{D}\Delta + \nu_T''(\mathcal{D}^2 + k^2), \\ \mathcal{L}_{SQ} &= -ik_x\boldsymbol{U} + \nu_T\Delta + \nu_T'\mathcal{D}. \end{aligned} \tag{9}$$

To build the linear estimators using LNS and eLNS, statistically converged velocity correlations are required. To obtain these correlations, the Lyapunov equations are derived from the equations written in the Orr-Sommerfeld Squire form as [Hwang and Cossu, 2010]

$$\begin{aligned} \mathbf{A}(k_x,k_y)\mathbf{X}(k_x,k_y) + \mathbf{X}(k_x,k_y)\mathbf{A}(k_x,k_y)^* \\ = -\mathbf{B}(k_x,k_y)\mathbf{B}(k_x,k_y)^*. \end{aligned} \tag{10}$$

The adjoint * here is defined with respect to the inner product $\langle \boldsymbol{u1}, \boldsymbol{u2} \rangle = \int_{-h}^{h} \boldsymbol{u1}^H \boldsymbol{u2} dz$. The matrix **X** gives the correlations $\langle \hat{\boldsymbol{q}}\hat{\boldsymbol{q}}^H \rangle$, and $\langle \hat{\boldsymbol{u}}\hat{\boldsymbol{u}}^H \rangle$ are obtained using the expression $\mathbf{CXC}^*$.

DNS Dataset

The Direct Numerical Simulation (DNS) dataset for an incompressible turbulent channel flow at a friction Reynolds number $Re_\tau = 2000$ is obtained from the Polytechnic University of Madrid (UPM) [Encinar et al., 2018]. The streamwise and spanwise directions have dimensions $8\pi \times 3\pi$. The DNS was performed on a grid with $2048 \times 2048 \times 512$ points in the streamwise, spanwise and wall-normal directions and the data were saved in Fourier space on a grid of size $512 \times 512 \times 512$. The range of wavenumbers available are $|k_x| = 0.25 - 8.0$ $(|\lambda_x| = 0.8 - 25)$ and $|k_y| = 0.66 - 21.0$ $(|\lambda_y| = 0.3 - 9.5)$. The 1146 instances in time for which the data are available ensures convergence of the 2-D energy spectrum.

Spectral Linear Stochastic Estimation

An estimator is built using the linear models and spectral linear stochastic estimation (SLSE) to estimate the flow fields. The estimator uses the streamwise velocity signal or the 2-D energy spectrum at a wall height z_2, to estimate the same quantity at a different wall height z_1. Before showing the results, we briefly review SLSE here following Baars et al. [2016].

For SLSE, a complex valued linear transfer kernel H_L is defined that takes as input the Fourier coefficient of the streamwise velocity at one wavenumber pair (k_x,k_y) and a wall-height z_2 $(\hat{u}(z_2;k_x,k_y))$, and estimates the same quantity at a wall-height z_1 $(\hat{u}'(z_1;k_x,k_y))$. Hence

$$\hat{u}'(z_1;k_x,k_y) = H_L(z_1,z_2;k_x,k_y)\hat{u}(z_2;k_x,k_y), \tag{11}$$

where the $'$ represents the estimated quantity. From (11), we see that to estimate the energy spectrum using SLSE, only the magnitude of H_L is required. Hence

$$\phi'_{uu}(z_1;k_x,k_y) = |H_L(z_1,z_2;k_x,k_y)|^2 \phi_{uu}(z_2;k_x,k_y), \tag{12}$$

where $\phi_{uu}(z;k_x,k_y)$ represents the 2-D energy spectrum of streamwise velocity at a wall height z. Multiplying (11) with the complex-conjugate of $\hat{u}(z_2;k_x,k_y)$ and taking an ensemble average (denoted by $\langle . \rangle$) gives the transfer kernel H_L as

$$\begin{aligned} H_L(z_1,z_2;k_x,k_y) &= \frac{\langle \hat{u}(z_1;k_x,k_y)\hat{u}^*(z_2;k_x,k_y) \rangle}{\langle \hat{u}(z_2;k_x,k_y)\hat{u}^*(z_2;k_x,k_y) \rangle} \\ &= |H_L(z_1,z_2;k_x,k_y)| e^{i\psi(z_1,z_2;k_x,k_y)}. \end{aligned} \tag{13}$$

Here $\psi(z_1,z_2;k_x,k_y)$ represents the phase of H_L. The denominator in (13) is the 2-D energy spectrum at z_2 and the numerator is the complex-valued cross-spectrum between z_2 and z_1.

Only the scales that are coherent between z_1 and z_2 can be properly estimated using (11) and (12). But, $|H_L|$ can have non-zero gain factors for the incoherent scales, hence providing false estimates for these scales. These incoherent scales are filtered out by setting the gain of $|H_L|$ to zero. This necessitates the quantification of coherence. For this purpose, the linear coherence spectrum (LCS) was defined by Tinney et al. [2006]. The LCS, denoted by γ^2, gives the fraction of energy that is correlated between two signals and is defined as

$$\gamma^2(z_1,z_2;k_x,k_y) = \frac{|\langle \hat{u}(z_1;k_x,k_y)\hat{u}^*(z_2;k_x,k_y) \rangle|^2}{\langle |\hat{u}(z_1;k_x,k_y)|^2 \rangle \langle |\hat{u}(z_2;k_x,k_y)|^2 \rangle}. \tag{14}$$

The incoherent scales are now defined as the scales with $\gamma^2 < \gamma_T^2$, where γ_T^2 $(= 0.05$ for the present study) is a chosen threshold value. Provided γ_T^2 is kept sufficiently low, the exact choice of this threshold value does not have a significant effect on the results. The gain of the incoherent scales in $|H_L|$ is thus set to zero, to obtain a filtered transfer kernel $(H_L)_{filt}$ [Tinney et al., 2006, Baars et al., 2016] which is used for estimation in the following sections.

Results

To illustrate the linear model based SLSE, this section first considers the estimation of both the instantaneous streamwise velocity field and the 2-D energy spectrum of $\boldsymbol{u}$ at $z_1^+ \approx 100$, with the measurement carried out at $z_2^+ \approx 300$. To understand the estimation using the linear models, a benchmark is required against which the estimate can be compared. For this purpose, the estimation based on the DNS dataset is used. The velocity signals from DNS are used to obtain the correlations required to compute H_L using (13). Further, the LCS computed from the same data (using (14)) is used to filter the transfer kernel and hence obtain $(H_L)_{filt}$, and this is used for estimation. The estimate of the instantaneous velocity field obtained from DNS at $z_1^+ \approx 100$ using an input at $z_2^+ \approx 300$ is shown in figure 1(a). Figure 1(b) shows the corresponding 2-D energy spectrum (obtained using (12)), in the pre-multiplied form. From figure 1(b),

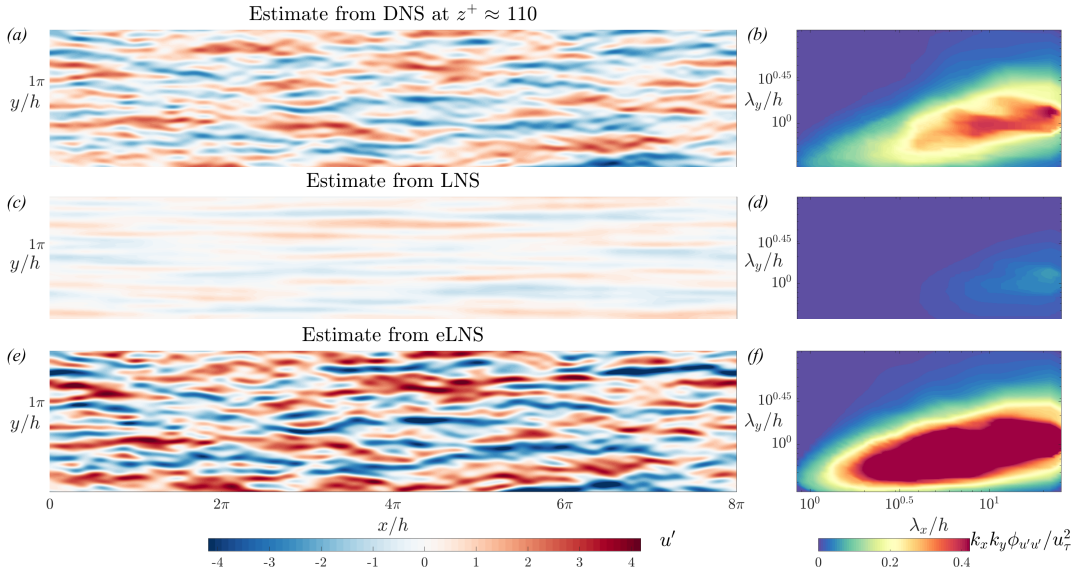

Figure 1: (a,c,e) The estimated instantaneous streamwise velocity field and (b,d,f) the corresponding 2-D energy spectrum obtained using (a,b) the DNS dataset, (c,d) LNS and (e,f) eLNS. The estimate is obtained at $z_1^+ \approx 100$ based on a measurement at $z_2^+ \approx 300$.

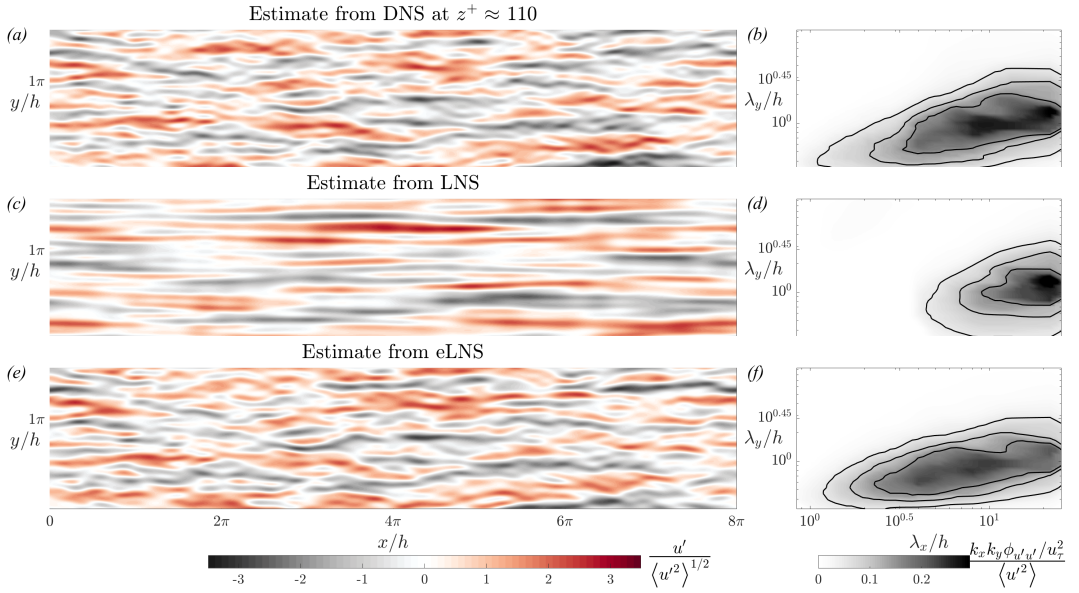

Figure 2: (a,c,e) The estimated instantaneous streamwise velocity field and (b,d,f) the corresponding 2-D energy spectrum obtained using (a,b) the DNS dataset, (c,d) LNS and (e,f) eLNS, normalised by $\langle u'^2 \rangle^{1/2}$ and $\langle u'^2 \rangle$ respectively. The estimate at $z_1^+ \approx 100$ based on a measurement at $z_2^+ \approx 300$ is shown. The contour lines in (b,d,f) correspond to $(k_x k_y \phi_{u'u'}/u_\tau^2)/\langle u'^{+2} \rangle = 0.05, 0.1$ and 0.15.

we see that the large scales are energetic in the estimate.

Now we consider the estimation using the linear models. Instead of directly using the velocity signals from the model, the correlations required for (13) and (14) are obtained from the solution to the Lyapunov equation (equation (10)). The transfer kernel $(H_L)_{filt}$ is obtained from both LNS and eLNS, and used to estimate the instantaneous streamwise velocity field and the 2-D energy spectrum. Figures 1(c) and 1(e) shows the estimates of instantaneous streamwise velocity obtained at $z_1^+ \approx 100$ using a measurement at $z_2^+ \approx 300$ using LNS and eLNS respectively. From these estimated velocity fields we see that the magnitude of u' is not obtained correctly by either of the models. This is also reflected in the estimated 2-D energy spectra in figures 1(d) and 1(f), where LNS underestimates the energy of the large scales while eLNS overestimates it for this combination of z_1 and z_2.

From figure 1(e) we see that, except for the actual magnitudes, the large-scale flow features modelled by eLNS are similar to DNS. To clarify this argument further, we normalise the estimated streamwise velocity and the energy spectra by $\langle u'^2 \rangle^{1/2}$ and $\langle u'^2 \rangle$ respectively. The normalisation factor is computed separately for DNS, LNS and eLNS by integrating the estimated energy spectra. Figure 2 shows the corresponding normalised estimates for those in figure 1.

Considering the estimate from LNS in comparison to DNS, we see from figure 2(c) that the estimate from LNS do not correspond to that obtained from DNS. This model only estimates

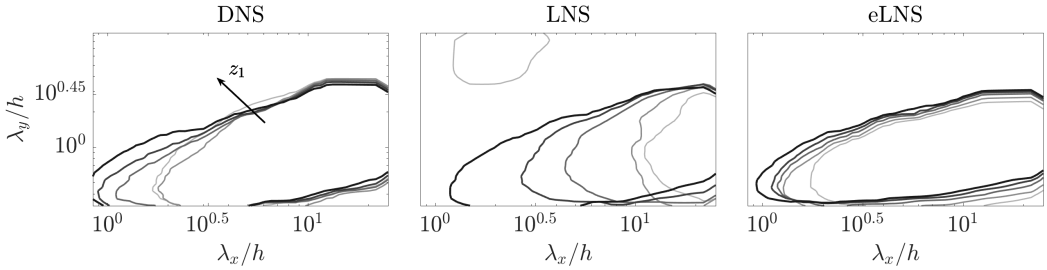

Figure 3: The contours corresponding to $(k_x k_y \phi_{u'u'}/u_\tau^2)/\langle u'^{+2}\rangle = 0.05$ from (a) DNS, (b) LNS and (c) eLNS for $z_1^+ \approx [200, 150, 100, 50, 10]$ and $z_2^+ \approx 300$.

the very large scales. This is also seen in the estimated energy spectrum, where only the largest scales remain energetic.

However, with the addition of the eddy viscosity model, as in eLNS, the large-scale structures in the instantaneous velocity estimate in figure 2(e) qualitatively resembles those from DNS. From the estimated energy spectrum in figure 2(f) we see that the relative distribution of energy among the large-scale structures, i.e. the shape of the pre-multiplied energy spectrum, is captured reasonably well by the model.

Varying the estimation location

So far only one estimation location of $z_1^+ \approx 100$ was considered. To investigate the quality of estimation over a range of wall-normal locations, we now consider multiple estimation locations in the inner-region of the flow at $10 < z_1^+ < 200$, as shown in figure 3. In this figure the energy spectra are normalised by the variance, as previously shown in figure 2. Each contour level corresponds to $(k_x k_y \phi_{u'u'}/u_\tau^2)/\langle u'^{+2}\rangle = 0.05$ at a particular z_1 from DNS, LNS and eLNS respectively. The contour lines get thicker and darker as z_1 moves away from the wall and closer to z_2.

From the estimates corresponding to LNS in figure 3, we see that the model reasonably obtains the shape of the spectra when z_1 is close to z_2. But the energetic region in the estimated spectrum diminishes rapidly as z_1 moves away from z_2 and closer to the wall. This is due to the critical layer behaviour of the LNS model [McKeon and Sharma, 2010] which models structures that are highly localised in the wall-normal direction and that are hence coherent only over narrow wall-normal distances. On the other hand, the estimates from eLNS remain energetic as z_1 moves away from z_2. Additionally, the relative distribution of energy among the large-scale motions of the flow, i.e the shape of the energy spectrum, is captured reasonably well by eLNS for a wide range of z_1. This indicates that, with the addition of an eddy viscosity profile, the structures diffuse in the wall-normal direction and are coherent over greater wall-normal distances. It should be noted that we can expect to obtain a good estimate from eLNS only when coherence between z_1 and z_2 is approximately captured by the model.

Conclusions

The main objective of this work was to build a linear estimator for a turbulent channel flow, using the linearized Navier-Stokes equations subject to stochastic forcing. Two variations of the linearized Navier-Stokes equations are considered: i) LNS, where the viscosity is equal to the kinematic viscosity and ii) eLNS, where the kinematic viscosity is augmented with an eddy viscosity profile. The estimator is built from each of these models using spectral linear stochastic estimation (SLSE). The estimator takes as input the data (streamwise velocity or the 2-D energy spectrum) at a wall height z_2 and provides an estimate at a different wall-height z_1. The estimation of both the instantaneous velocity field and the 2-D energy spectra has been considered.

The estimates obtained from the models are compared to those obtained from SLSE carried out using direct numerical simulation data of a turbulent channel flow at $Re_\tau = 2000$. The comparison is based on two factors, i) the magnitude of the estimated velocity fluctuations and ii) the relative distribution of the large-scale motions. From the estimated velocity fields and the corresponding energy spectra, we observe that both LNS and eLNS do not estimate the magnitude of the streamwise velocities correctly. As a result, the magnitude of energy in the 2-D energy spectrum is also not estimated correctly by the models. Additionally, the range of energetic scales estimated by LNS diminishes rapidly as the estimation location moves away from the measurement location. However, eLNS captures the range of wavelengths that are energetic. eLNS also obtains the relative distribution of energy among these large-scale motions reasonably well, for a range of estimation locations.

Acknowledgements

The financial support of the Australian Research Council is gratefully acknowledged.

References

W. J. Baars, N. Hutchins, and I. Marusic. Spectral stochastic estimation of high-Reynolds-number wall-bounded turbulence for a refined inner-outer interaction model. *Phys. Rev. Fluids*, 1:054406, 2016.

R. D. Cess. A survey of the literature on heat transfer in turbulent tube flow. *Res. Rep*, pages 8 – 0529, 1958.

J. C. Del Álamo and J. Jiménez. Linear energy amplification in turbulent channels. *J. Fluid Mech.*, 559:205213, 2006.

M. P. Encinar, A. Vela-Martín, A. García-Gutiérrez, and J. Jiménez. A second-order consistent, low-storage method for time-resolved channel flow simulations. *ArXiv e-prints*, Aug. 2018.

Y. Hwang and C. Cossu. Linear non-normal energy amplification of harmonic and stochastic forcing in the turbulent channel flow. *J. Fluid Mech.*, 664:51–73, 2010.

B. J. McKeon and A. S. Sharma. A critical-layer framework for turbulent pipe flow. *J. Fluid Mech.*, 658:336-382, 2010.

W. C. Reynolds and A. K. M. F. Hussain. The mechanics of an organized wave in turbulent shear flow. Part 3. Theoretical models and comparisons with experiments. *J. Fluid Mech.*, 54(02):263-288, 1972.

C. E. Tinney, F. Coiffet, J. Delville, A. M. Hall, P. Jordan, and M. N. Glauser. On spectral linear stochastic estimation. *Exp. Fluids*, 41(5):763-775, 2006.